ChemComm

Accepted Manuscript

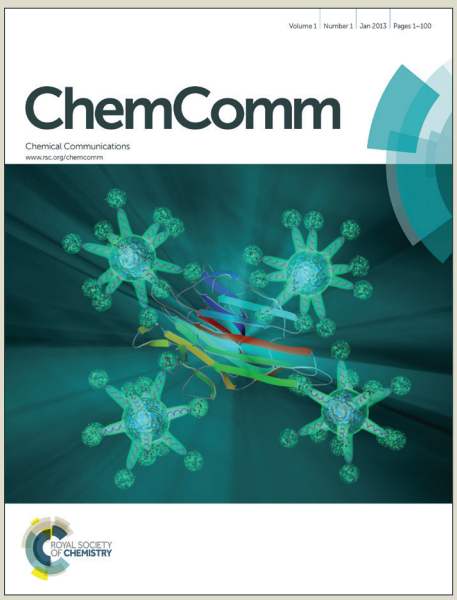

ROYAL SOCIETY OF CHEMISTRY

www.rsc.org/chemcomm

ChemComm

COMMUNICATION

Silica shelled and block copolymer encapsulated red-emissive AIE nanoparticles with 50% quantum yield for two-photon excited vascular imaging†

Received 00th January 20xx,
Accepted 00th January 20xx

DOI: 10.1039/x0xx00000x

www.rsc.org/

Junlong Geng,[ab] Chi Ching Goh,[c] Wei Qin,[d] Rongrong Liu,[b] Nikodem Tomczak,[b] Lai Guan Ng,[c] Ben Zhong Tang,[de] and Bin Liu*[ab]

A polymer and silica co-protection strategy has been developed to encapsulate organic fluorogens with aggregation-induced emission and charge transfer characteristics into small nanoparticles (NPs). The co-pretected NPs show bright red fluorescence (50% quantum yield) with a large two-photon action cross-section (450 GM at 840 nm), which have been sucessfully used for two-photon fluorescence imaging of vasculature of the mouse tibial muscle.

Two-photon microscopy is a powerful technique for three-dimensional study of complicated biological processes. As compared to one-photon excited technique, two-photon fluorescence imaging (TPFI) demonstrates advantages in high penetration depth, minimized phototoxicity, and less autofluorescence due to the utilization of near infrared laser (700–1000 nm).[1] To achieve a high signal-to-noise ratio in TPFI, two-photon absorbing materials should have a large two-photon action cross section, which is the product of the fluorescence quantum yield (η) and the two-photon absorption (TPA) cross section (δ). Currently, the most popular TPA materials are conjugated organic molecules.[2] An effective strategy to increase δ is to design strong donor-acceptor structures, which have a large excited state intramolecular charge transfer (ICT) character.[3] However, once these ICT molecules are transferred from organic solvents to aqueous media through either nanoparticle (NP) formulation or side chain modification,[1c,2d,4] their $\eta\delta$ values decrease significantly, primarily due to the significant drop in η. This is largely due to aggregation-caused quenching (e.g. π-π stacking of molecules) and environmental quenching (e.g. oxygen and polar media). To tackle this issue, fluorogens with aggregation-induced emission characteristics (AIEgen) have been developed to offer organic fluorophore based NPs with high η in water.

AIEgens usually show weak fluorescence as molecular species due to free intramolecular rotation, and they exhibit strong emission in aggregated states as a result of the restriction of free motion.[5] Tetraphenylethylene (TPE, Scheme 1A) is a typical AIEgen. The free rotation of phenyl groups makes it very weakly fluorescent in tetrahydrofuran (THF) but emits strong fluorescence in the solid state.[6] More interestingly, attachment of TPE groups to existing fluorogens could enable them with typical AIE properties. For example, conjugating TPE with ICT fluorophores could yield fluorogens with both AIE and ICT characteristics. TPETPAFN is a typical fluorogen consisting of two TPE pendants (AIE active groups) and an ICT core. This AIE and ICT conjugation strategy renders TPETPAFN with a high far red/near infrared emission and an η of ~20% in aqueous media as NPs.[3a,7] However, the η of TPETPAFN loaded NPs is still much lower than that in solid state (η = 52%). As such, an efficient strategy to enhance η of ICT based fluorogens in aqueous media is highly sought after.

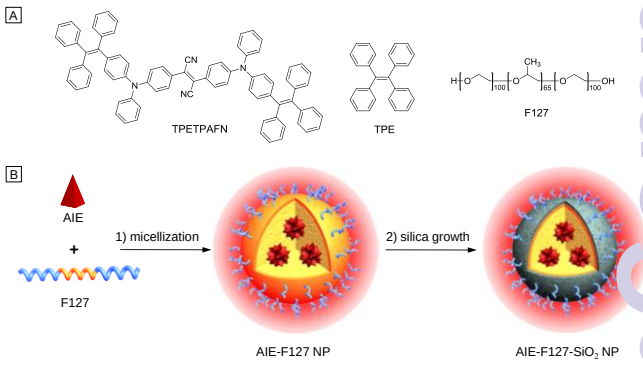

Scheme 1 (A) Chemical structures of TPETPAFN, TPE and F127. (B) The synthesis of AIE-F127 NPs and AIE-F127-SiO_2 NPs.

Several matrices (e.g. lipid based block copolymers, poly (DL-lactide-*co*-glycolide), bovine serum albumin, and F127) have been utilized to encapsulate AIEgens to yield AIE NPs, exhibiting excel

[a] *Department of Chemical and Biomolecular Engineering, National University of Singapore, Singapore 117585*
E-mail: cheliub@nus.edu.sg
[b] *Singapore Immunology Network (SIgN), A*STAR (Agency for Science, Technology and Research), Biopolis, Singapore 138648*
[c] *Institute of Materials Research and Engineering, 3 Research Link, Singapore 117602*
[d] *Department of Chemistry, Division of Biomedical Engineering, The Hong Kong University of Science and Technology, Clear Water Bay, Kowloon, Hong Kong, China*
[e] *SCUT-HKUST Joint Research Laboratory, Guangdong Innovative Research Team, State Key Laboratory of Luminescent Materials & Devices, South China University of Technology, Guangzhou 510640, China*
† Electronic supplementary information (ESI) available: experimental section and results. See DOI: 10.1039/x0xx00000x

performance in biological sensing and imaging applications.[7c,8] Moreover, the η of AIE NPs could be further optimized by modulating polymer matrices, AIEgen packing states and their loading concentrations.[8e,9] For example, Wu et. al. reported that the η of AIE NPs prepared using poly(ethylene glycol)-*b*-poly(styrene) (PEG-*b*-PS) is higher than that of poly(ethylene glycol)-*b*-poly(e-caprolactone) (PEG-*b*-PCL), which is ascribed to the increased hydrophobicity of PS as compared to PCL.[9b] In addition to polymer matrices, silica has been widely utilized to encapsulate conventional and AIEgens to improve their fluorescence performance.[10] Fluorogen loaded silica NPs exhibit improved brightness and photostability thanks to the separation of organic fluorogens from quenchers (e.g. water, oxygen) by silica matrices.[11] The positive effects of both polymer and silica protection on organic fluorogens motivated us to improve the η of ICT fluorogen loaded NPs through a polymer/silica co-protection approach.

In this communication, we report a simple strategy to enhance $\eta\delta$ and stability of ICT fluorogen based NPs. Taking TPETPAFN as an example, AIEgens were encapsulated into F127 matrices to yield TPETPAFN-F127 NPs, which were further coated with a silica layer to yield TPETPAFN-F127-SiO_2 NPs. Interestingly, the η of TPETPAFN-F127-SiO_2 NPs was improved nearly 100% relative to that of TPETPAFN-F127 NPs, and the reason was revealed by both static and dynamic photoluminescence (PL) studies. In addition, individual NP brightness was also compared against commercial quantum dot (QD655). At last, the obtained TPETPAFN-F127-SiO_2 NPs have been successfully used to visualize blood vasculature of the mouse tibial muscle *via* real-time TPFI.

TPETPAFN was synthesized according to the previous reports (**Scheme 1**A).[7c,8e] The AIE characteristics of both TPETPAFN and TPE were investigated by examining their emission spectra changes in THF/water mixture at different water fractions (f_w). At lower f_w, TPETPAFN and TPE show weak fluorescence, while their fluorescence intensities increase obviously with an increase of f_w. When f_w reaches 90%, the corresponding fluorescence intensities of TPETPAFN and TPE are increased up to 70-fold and 86-fold, respectively, as shown in Fig. S1 in the supporting information (SI). In addition, the solvent effects on the absorption and emission spectra have also been studied (Fig. S2). With increasing solvent polarity, the emission maximum of TPETPAFN is red-shifted from 597 nm in hexane to 643 nm in toluene and 652 nm in THF, accompanied with fluorescence intensity decrease. The large fluorescence change of TPETPAFN in different solvents demonstrates its strong ICT character. On the other hand, the emission spectra of TPE remain nearly the same in different solvents as shown in Fig. S2B, illustrating its weak ICT property.

The AIEgen loaded NPs were prepared in one-step using a triblock copolymer of F127 (a commercial polymer) as the encapsulation matrix (Scheme 1B).[12] It started with the preparation of a THF solution of F127 and AIEgens. The solution was then blow dried with nitrogen and further sonicated in water to yield AIEgen loaded F127 NPs (AIE-F127 NPs). Accordingly, the TPETPAFN loaded F127 NPs are denoted as TPETPAFN-F127 NPs while TPE loaded F127 NPs are denoted as TPE-F127 NPs. The obtained AIE-F127 NPs were further coated with a silica shell by a sol-gel procedure.[12b] The thin silica shell was optimized through addition of diethoxydimethylsilane (DEDMS) into the NP suspension, which helps quench the silicate cross-linking (Scheme 1B). The product mixtures were then dialyzed to yield silica cross-linked and F127 encapsulated NPs (TPE-F127-SiO_2 NPs and TPETPAFN-F127-SiO_2 NPs).

TPETPAFN-F127 NPs exhibit small black dots with a size around ~5 nm under the FE-TEM (Fig. S3A). After coating a silica layer, TPETPAFN-F127-SiO_2 NPs have a relatively uniform size of ~12 nm (Fig. S3B). In addition, the sizes of both NPs have been investigated with dynamic light scattering (DLS) technique, which are ~32 nm and ~25 nm for TPETPAFN-F127 NPs and TPETPAFN-F127-SiO_2 NPs, respectively (Fig. S3C). The respective sizes of TPE-F127 NPs and TPE-F127-SiO_2 NPs are similar to those of TPETPAFN-F127 NPs and TPETPAFN-F127-SiO_2 NPs (data not shown). The sizes of TPETPAFN-F127-SiO_2 NPs remain constant for the tested period (10 days), demonstrating their excellent colloidal stability (Fig. S4).

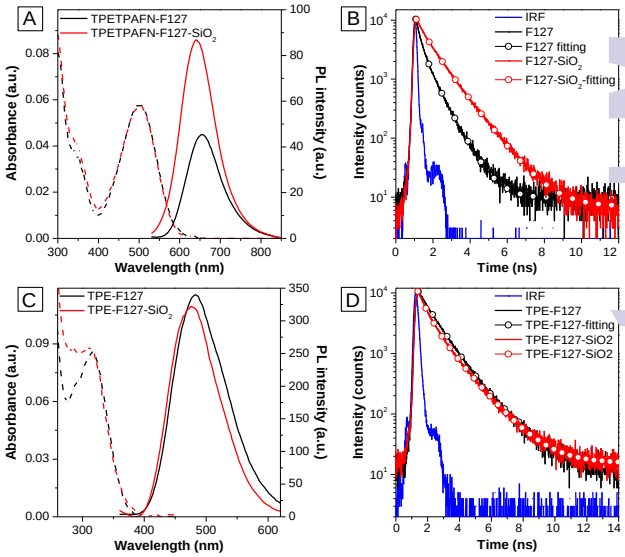

Fig. 1 The absorption (dash-dotted lines) and PL (solid lines) spectra of (A) TPETPAFN-F127 NPs (black) and TPETPAFN-F127-SiO_2 NPs (red), and (C) TPE-F127 NPs (black) and TPE-F127-SiO_2 NPs (red). The emission decay curves of (B) TPETPAFN-F127 NPs (black), TPETPAFN-F127-SiO_2 NPs (red); (D) TPE-F127 NPs (black), TPE-F127-SiO_2 NPs (red). The instrument response (IRF) (blue) signal is also shown for reference in B and D.

Fig. 1A shows the UV-vis absorption and PL spectra of TPETPAFN-F127 NPs and TPETPAFN-F127-SiO_2 NPs in water. Both NP suspensions exhibit similar absorption maxima at ~ 500 nm. Although they have similar absorbance, TPETPAFN-F127-SiO_2 NPs (η = 50 ± 1%) display much higher brightness than that of TPETPAFN-F127 NPs (24 ± 1%). In addition, as shown in Fig. 1B, the emission maxima for TPETPAFN-F127-SiO_2 NPs and TPETPAFN-F127 NPs are located at 641 nm and 655 nm, respectively. The blue-shifted emission maximum with silica layer indicates less polar environment in the F127/silica matrix as compared to F127 alone.[7c,13] To the best of our knowledge, the 50 ± 1% is the highest η for the reported TPETPAFN NPs,[7c,8c,8e,9b] which is similar to that in solid state (η = 52%).[7c] On the other hand, as shown in Figure 1C, at the same absorbance, the emission of TPE-F127-SiO_2 NPs (η = 23 ± 1%) is similar to that of TPE-F127 NPs (η = 21 ± 1%). No obvious fluorescence enhancement has been observed for TPE based NPs with and without SiO_2 coating, which is very different from that of TPETPAFN NPs. As shown in Fig. S2, TPETPAFN emits strong fluorescence in non-polar solvents but it is very weakly emissive in

polar media. The protective silica layer thus provides a relatively less polar environment for TPETPAFN by minimizing its contact with water. However, the environmental polarity change does not influence the fluorescence of TPE (Fig. S2), which agrees with the very minor fluorescence change for TPE NPs with and without silica coating.

To understand the effect of silica coating on fluorescence, the fluorescence lifetimes for all the synthesized NPs were examined with a Fluorolog-3 iHR spectro-fluorometer. The relationship between η and fluorescence lifetime (τ) of a fluorophore is given by $\eta = \Gamma/(\Gamma + k_{nr})$ and $\tau = (\Gamma + k_{nr})^{-1}$,[14] where Γ and k_{nr} are radiative decay and nonradiative decay rates, respectively. The Γ is the intrinsic property of a fluorophore, which is generally regarded as a constant. The changes of η and τ are thus mainly resulted from the variation in k_{nr}. In addition, the η and τ values are expected to vary in the same direction, either both increase or both decrease based on the above equations.[14] Fig. 1B shows the fluorescence lifetime decay curves of TPETPAFN-F127-SiO_2 NPs and TPETPAFN-F127 NPs. Clearly, the average fluorescence lifetime of TPETPAFN-F127-SiO_2 NPs (4.18 ns, Table S1) is more than twice longer relative to that of TPETPAFN-F127 NPs (1.81 ns, Table S1). The longer lifetime of TPETPAFN-F127-SiO_2 NPs should be due to blocking of nonradiative decay pathways of TPETPAFN fluorogens in the aggregated state. The silica layer in TPETPAFN-F127-SiO_2 NPs should also prevent the contact between TPETPAFN and water/oxygen molecules, both are beneficial to the fluorescence enhancement. On the other hand, TPE-F127-SiO_2 NPs and TPE-F127 NPs have a similar average fluorescence lifetime (4.99 vs 5.23 ns, Table S1), which is consistent with the close η for both.

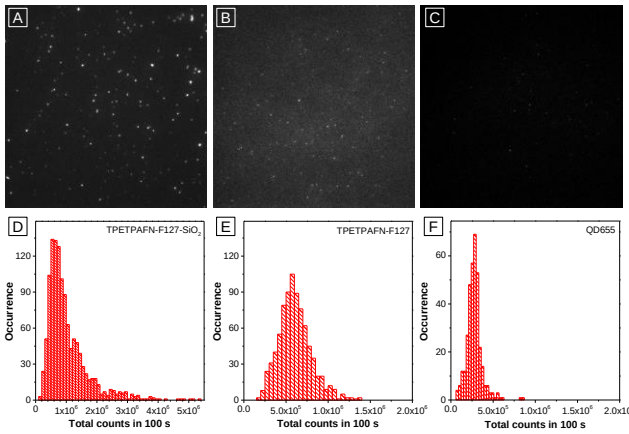

Fig. 2 (A, B, C) Wide field fluorescence images and (D, E, F) histograms of the total numbers of photons collected for (A, D) TPETPAFN-F127-SiO_2 NPs, (B, E) TPETPAFN-F127 NPs and (C, F) commercial QD655. Note the different binning and scales for D, E and F; λ_{ex} = 488 nm for all samples.

The fluorescence behaviours of TPETPAFN-F127-SiO_2 NPs and TPETPAFN-F127 NPs were subsequently investigated using single NP fluorescence imaging. The commercial QD655 with a diameter around ~20 nm (based on DLS measurement) was chosen as the reference. Typical single NP fluorescence images of TPETPAFN-F127-SiO_2 NPs, TPETPAFN-F127 NPs, and QD655 are shown in Fig. 2A-C, respectively. The emission of TPETPAFN-F127-SiO_2 NPs is obviously brighter than that of TPETPAFN-F127 NPs and QD655. The intensity time-traces of TPETPAFN-F127-SiO_2 NPs, TPETPAFN-F127 NPs and QD655 were recorded over 100 s. As shown in Fig. 2D-F, the average number of photons emitted by each TPETPAFN-F127-SiO_2 NP (1.04×10^6 counts) is around 1.7-fold of TPETPAFN-F127 NP (6.08×10^5 counts), and 3.7-fold of commercial QD655 (2.8×10^5 counts). The trend is similar to their overall fluorescence intensities measured by a fluorometer. In addition, fluorescence intensity time traces for individual NP reveal that both TPETPAFN-F127-SiO_2 NPs and TPETPAFN-F127 NPs keep stable fluorescence, while QD 655 shows prominent fluorescence intermittency, which is referred to as blinking (Fig. S5). It is also worth noting that the photostability of TPETPAFN-F127-SiO_2 is better than that of TPETPAFN-F127 NPs upon continuous laser excitation (Fig. S6), which should result from the protection of silica layer. Considering the similar DLS size of TPETPAFN-F127-SiO_2 NPs (~25 nm) and TPETPAFN-F127 NPs (~3 nm) with that of QD655 (~20 nm), the higher brightness and more stable TPETPAFN-F127-SiO_2 NPs are thus promising for biological applications.

Excellent signal stability of fluorescent probes is of high importance for biological applications. As a result, the fluorescence intensity changes were studied for TPETPAFN-F127-SiO_2 NPs upon incubation in 1 × PBS at 37 °C for 10 days. No evident fluorescence change indicates good physical stability of the NPs (Fig. S7A and its inset). On the other hand, the cytotoxicity results of the NIH/3T3 fibroblast cells upon incubation with 100 to 500 μg/mL of TPETPAFN-F127-SiO_2 NPs are shown in Fig. S7B. The cell viabilities are > 90% after 48 h, demonstrating their low cytotoxicity, which is desirable for biological imaging.

Real-time visualization of blood vessels *in vivo* is important to study biological processes, for instance, vascular leakage, angiogenesis, and leukocyte extravasation.[15] As compared to one photon excited fluorescence imaging, TPFI is often used for the visualization of tissues or vessels due to the use of near infrared excitation which offers deeper tissue penetration, in addition to low autofluorescence interference and minimal phototoxicity to biosubstrates. Materials with large δ values are thus desirable to achieve high imaging contrast. The TPA spectra of TPETPAFN-F127-SiO_2 NPs in water were investigated together with Evans Blue, a widely used TPA contrast agent in vascular imaging.[16] The δ of TPETPAFN-F127-SiO_2 NPs was analyzed based on NP concentration and the corresponding TPA spectrum is shown in Fig. S8. The TPETPAFN-F127-SiO_2 NPs show a maximum δ of 900 GM at 84 nm,[17] which is considerably better than Evans Blue.

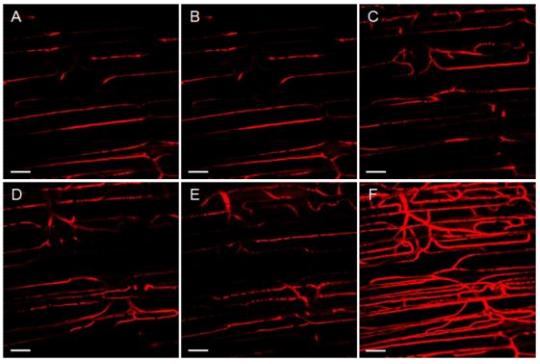

Fig. 3 Intravital TPFI for blood vessels of mouse tibial muscle stained with TPETPAFN-F127-SiO_2 NPs at depths of (A) 0, (B) 20, (C) 40, (D) 60, (E) 80 μm and (F) the respective Z-projected image. The scale bar is 50 μm.

The biological application of TPETPAFN-F127-SiO_2 NPs was subsequently explored. After intravenous administration of the NPs to an anaesthetized mouse, the vasculature of the tibial muscle was imaged using a two-photon microscopy.[16] Fig. 3A–E shows representative images of the blood vessels at different depths. Both major blood vessels and smaller capillaries of the tibial muscle are clearly visualized because of TPETPAFN-F127-SiO_2 NPs, with no obvious aggregation of NPs observed. It also shows 1.6-fold higher fluorescence signal than that upon injection with TPETPAFN-F127 NPs at the same concentration for TPETPAFN (Fig. S9 in SI). Under the same imaging condition, no fluorescent signal is detected without NP administration (Fig. S10 in SI). The Z-projected (Fig. 3F) image illustrates that the NPs could effectively label the vasculature in vivo.

In summary, a F127-silica co-encapsulation strategy has been developed to improve the η of ICT fluorogen based NPs using TPETPAFN as an example. The obtained TPETPAFN-F127-SiO_2 NPs have a QY of 0.50 as a result of the relatively non-polar microenvironment provided by the silica shell and the reduced water and oxygen attack to TPETPAFN. Single NP study proves that the TPETPAFN-F127-SiO_2 NPs exhibit higher brightness and better photostability as compared to TPETPAFN-F127 NPs. The large $\eta\delta$ value and excellent biocompatibility make TPETPAFN-F127-SiO_2 NPs a good contrast agent for two-photon *in vivo* blood vascular imaging, as illustrated using the tibial muscle model. The polymer and silica shell dual encapsulation strategy is expect to help improve the performance of ICT fluorogen loaded NPs in various fluorescence imaging applications.

We thank Singapore NRF Investigatorship (R279-000-444-281) and the JCO (IMRE/14-8P1110), the Research Grants Council of Hong Kong (604913, 16301614, N_HKUST620/11 and N_HKUST604/14) and Guangdong Innovative Research Team Program (201101C0105067115) for financial support.

Notes and references

1. (a) S. A. Sanchez, E. Gratton, *Acc. Chem. Res.*, 2005, **38**, 469; (b) P. T. C. So, C. Y. Dong, B. R. Masters, K. M. Berland, *Annu. Rev. Biomed. Eng.*, 2000, **2**, 399; (c) G. S. He, L. S. Tan, Q. Zheng, P. N. Prasad, *Chem. Rev.*, 2008, **108**, 1245; (d) F. Helmchen, W. Denk, *Nat. Methods*, 2005, **2**, 932; (e) C. Xu, W. Zipfel, J. B. Shear, R. M. Williams, W. W. Webb, *Proc. Natl. Acad. Sci. U.S.A.*, 1996, **93**, 10763; (f) D. R. Larson, W. R. Zipfel, R. M. Williams, S. W. Clark, M. P. Bruchez, F. W. Wise, W. W. Webb, *Science*, 2003, **300**, 1434.
2. (a) S. Kim, H. E. Pudavar, A. Bonoiu, P. N. Prasad, *Adv. Mater.*, 2007, **19**, 3791; (b) H. Ma, A. K. Y. Jen, *Adv. Mater.*, 2001, **13**, 1201; (c) B. A. Reinhardt, L. L. Brott, S. J. Clarson, A. G. Dillard, J. C. Bhatt, R. Kannan, L. X. Yuan, G. S. He, P. N. Prasad, *Chem. Mater.*, 1998, **10**, 1863; (d) H. Y. Woo, B. Liu, B. Kohler, D. Korystov, A. Mikhailovsky, G. C. Bazan, *J. Am. Chem. Soc.*, 2005, **127**, 14721.
3. (a) R. Hu, E. Lager, A. Aguilar-Aguilar, J. Liu, J. W. Y. Lam, H. H. Y. Sung, I. D. Williams, Y. Zhong, K. S. Wong, E. Peña-Cabrera, B. Z. Tang, *J. Phys. Chem. C*, 2009, **113**, 15845; (b) A. Bhaskar, G. Ramakrishna, Z. Lu, R. Twieg, J. M. Hales, D. J. Hagan, E. Van Stryland, T. Goodson, *J. Am. Chem. Soc.*, 2006, **128**, 11840; (c) S. J. K. Pond, O. Tsutsumi, M. Rumi, O. Kwon, E. Zojer, J.-L. Brédas, S. R. Marder, J. W. Perry, *J. Am. Chem. Soc.*, 2004, **126**, 9291; (d) K. P. Divya, S. Sreejith, P. Ashokkumar, K. Yuzhan, Q. Peng, S. K. Maji, Y. Tong, H. Yu, Y. Zhao, P. Ramamurthy, A. Ajayaghosh, *Chem. Sci.*, 2014, **5**, 3469; (e) Y. F. Feng, Y. L. Yan, S. Wang, W. H. Zhu, S. X. Qian, H. *J.* Tian, *Mater. Chem.*, 2006, **16**, 3685.
4. J. L. Geng, K. Li, D. Ding, X. H. Zhang, W. Qin, J. Z. Liu, B. Z. Tang, B. Liu, *Small*, 2012, **8**, 3655.
5. (a) Y. N. Hong, J. W. Y. Lam, B. Z. Tang, *Chem. Commun.*, 2009, 4332; (b) D. Ding, K. Li, B. Liu, B. Z. Tang, *Acc. Chem. Res.*, 2013, **46**, 2441; (c) Z. Chi, X. Zhang, B. Xu, X. Zhou, C. Ma, Y. Zhang, S. Liu, J. Xu, *Chem. Soc. Rev.*, 2012, **41**, 3878-3896. (d) Liang, J.; Tang, B. Z.; Liu, B. Chem. Soc. Re 2015; DOI:10.1039/C4CS00444B.
6. (a) J. Zhao, D. Yang, Y. X. Zhao, X. J. Yang, Y. Y. Wang, B. Wu, *Angew. Chem. In. Ed.*, 2014, **53**, 6632; (b) J. Zhao, J. W. Y. Lam, B. Z. Tang, *J. Mater. Chem.*, 2012, **22**, 23726.
7. (a) K. Li, B. Liu. *Chem. Soc. Rev.* 2014, **43**, 6570-6597; (b) D. Wang, L. Qian, W. Qin, A. J. Qin, B. Z. Tang, S. L. He, *Sci. Rep.*, 2014, **4**, 4279; (c) K. Li, W. Qin, D. Ding, N. Tomczak, J. L. Geng, R. R. Liu, J. Z. Liu, X. H. Zhang, H. W. Liu, B. Liu, B. Z. Tang, *Sci. Rep.*, 2013, **3**, 1150; (d) J. L. Geng, K. Li, W. Qin, B. Z. Tang and B. Liu *Part. Syn. Part. Charact*. 2014, **31**, 1238; (e) K. Li, Z. S. Zhu, P. Q. Cai, N. Tomczak, R. Liu, D. Ding, J. Liu, W. Qin, Z. Zhao, Y. Hu, X. D. Chen, B. Z. Tang, B. Liu *Chem. Mater.*, 2013, **25**, 4181; (f) K. Li, D. Ding, C. Prashant, W. Qin, C. T. Yang, B. Z. Tang, B. Liu. *Adv. Healthcare Mater.* 2013, **2**, 1600.
8. (a) Y. D. Lee, C. K. Lim, A. Singh, J. Koh, J. Kim, I. C. Kwon, S. Kim, *Acs Nano*, 2012, **6**, 6759; (b) W. Qin, D. Ding, J. Z. Liu, W. Z. Yuan, Y. Hu, B. Liu, B. Z. Tang, *Adv. Funct. Mater.*, 2012, **22**, 771; (c) J. L. Geng, Z. S. Zhu, W. Qin, L. Ma, Y. Hu, G. G. Gurzadyan, B. Z. Tang, B. Liu, *Nanoscale*, 2014, **6**, 939; (d) H. G. Lu, X. W. Zhao, W. J. Tian, Q. S. Wang, J. Shi, *Rsc Adv.*, 2014, **4**, 18460; (e) J. L. Geng, K. Li, W. Qin, L. Ma, G. G. Gurzadyan, B. Z. Tang, B. Liu, *Small*, 2013, **9**, 2012.
9. (a) W. C. Wu, C. Y. Chen, Y. Q. Tian, S. H. Jang, Y. N. Hong, Y. Liu, R. R. Hu, B. Z. Tang, Y. T. Lee, C. T. Chen, W. C. Chen, A. K. Y. Jen, *Adv. Funct. Mater.*, 2010, **20**, 1413;
10. (a) A. Burns, H. Ow, U. Wiesner, *Chem. Soc. Rev.*, 2006, **35**, 1028; (b) Y. M. Wang, X. X. He, X. H. Yang, H. Shi, *Acc. Chem. Res.*, 2013, **46**, 1367.
11. (a) S. Inagaki, O. Ohtani, Y. Goto, K. Okamoto, M. Ikai, K. Yamanaka, T. Tani, T. Okada, *Angew. Chem. In. Ed.*, 2009, **48**, 4042; (b) L. Wang, W. Tan, *Nano Lett.*, 2006, **6**, 84; (c) J. Geng, J. Liu, J. Liang, H. Shi, B. Liu, *Nanoscale*, 2013, **5**, 8593.
12. (a) J. L. Geng, C. C. Goh, N. Tomczak, J. Liu, R. R. Liu, L. Ma, L. G. Ng, G. G. Gurzadyan, B. Liu, *Chem. Mater.*, 2014, **26**, 1874; (b) Q. S. Huo, J. Liu, Q. Wang, Y. B. Jiang, T. N. Lambert, E. Fang, *J. Am. Chem. Soc.*, 2006, **128**, 6447.
13. Y. L. Cao, M. D. Yang, Y. Wang, H. P. Zhou, J. Zheng, X. Z. Zhang, J. Wu, Y. P. Tian, Z. Q. Wu, *J. Mater. Chem. C*, 2014, **2**, 3686.
14. J. R. Lakowicz, *Principles of Fluorescence Spectroscopy*, 3rd ed Springer: Berlin, 2006.
15. (a) C. D. Andrade, C. O. Yanez, H. Y. Ahn, T. Urakami, M. V. Bondar, M. Komatsu, K. D. Belfied, *Bioconjugate Chem.*, 2011, **22**, 2060; (b) A. Jayagopal, P. K. Russ, F. R. Haselton, *Bioconjugate Chem.*, 2007, **18**, 1424; (c) W. G. Roberts, G. E. Palade, *J. Cell Sci.*, 1995, **108**, 2369; (d) A. Sen Gupta, *Nanomed.-Nanotechnol.*, 2011, **7**, 763.
16. J. L. Li, C. C. Goh, J. L. Keeble, J. S. Qin, B. Roediger, R. Jain, Y. L. Wan, W. K. Chew, W. Weninger, L. G. Ng, *Nat. Protoc.*, 2012, **7**, 221.
17. D. A. Oulianov, I. V. Tomov, A. S. Dvornikov, P. M. Rentzepis, *Opt. Commun.*, 2001, **191**, 235.